Supplementary Materials
Molecular Biology of the Cell
Junker *et al*.

Figure S1. BB MTs display bending consistent with ciliary bending. (A) The A- and B-tubules of cilia are structurally continuous with the A- and B-tubules of the BB. The left image is a maximum-projected EM tomogram image showing BB triplet MTs continuous with its associated ciliary doublet MTs. The cortical cytoskeleton and plasma membrane flanks the cilium. Scale bar, 100 nm. Middle image is an inset from the tomogram defined by red box, the model to the right of the inset indicates the continuity of A- and B-tubules between the BB and the cilium. (B) Representative thin section EM images of unciliated and ciliated BBs and their respective bending profiles. Scale bar, 200 nm. n=37 BBs. (C) Images showing the method used to obtain curvature values for both BBs and cilia in thin section EM images that were quantified in Figure 1B. (D) Images showing the process used to obtain curvature values from both BBs and cilia in 3-dimensional EM tomograms. (E) The scatter plots of the distribution of BB and proximal cilium lengths contained in the EM thin sections (Figure 1B) and EM tomograms (Figures 2-6). (F) Comparison of MT curvature of BBs between two independent modelers - Author 1 (A. Junker) and Author 3 (A. Soh). Left panels show side views and top views of the same BB independently modeled. The graph on the right compares mean curvature values for each triplet obtained from each model, curvatures are consistently most prominent at triplet MTs 5 and 6. Asterisk denotes p-value <0.05. Heat maps below show distribution of curvature between independent models. Curvature is consistently most prominent near the base-middle of triplet MTs 5-6.

Figure S2. BBs bend consistent with ciliary beat stroke at 37°C. (A) BBs display different bending patterns depending on where the cilium is in the beat stroke. Left panels are 8.6 nm max-projected images of EM tomograms. Scale bar, 200 nm. The two middle panels on the left are model views (side and top views) of BB triplet MTs from the corresponding EM tomogram. Colors indicate curvature of the modeled triplet MTs where cold colors (blue) indicate low curvature and warm colors indicate high curvature (red). The two middle panels on the right are graphs showing BB curvature for the BB proximal to distal axis (left) or for each triplet MT (right). The maximum value for each bin (1/10th the length of the BB) along the BB proximal-distal axis is normalized by

subtracting the lowest maximum value of all bins in each BB. The graph represents the means and standard deviations of these normalized maximum values for each proximal to distal bin (left) or each triplet MT (right). BBs exhibit different bending profiles depending on the cilium's position in the beat cycle. Grey dots represent curvature values from individual bins, black lines indicate means, and error bars indicate the standard deviation. Right panels show curvature heatmaps of the positive and negative curvature for each proximal-distal bin in each triplet MT. Black "X's" indicate missing bins due to incomplete EM tomogram volumes. The blue and red colors indicate the direction of curvature relative to the cell's anterior-posterior axis (axis of the ciliary power stroke). Blue indicates negative bending which is towards the cell anterior. Red indicates positive bending which is towards the cell posterior. n = 6 BBs analyzed. (B) Heatmap indicate that the average curvatures for the WT BBs near the end and early recovery of the power stroke. n = 3 BBs at end / early recovery of the ciliary beat cycle. (C) Standard deviation of the average denotes the greatest deviations in triplet MTs 5 and 6. Scale bar, 200 nm.

Figure S3. Computational model of BB bending. (A) A computational (finite-element) model of the cilium, BB, SF, BB-appendage MTs, and cell cortex was generated in COMSOL Multiphysics using the Beam interface within the Structural Mechanics module. EM tomogram models (left) matched to the position of the cilium in the power stroke is compared to the computational model (right) and show consistent MT bending direction and similarly increased bending at triplet MTs 5-6. Model colors indicate curvature of the modeled triplet MTs where cold colors (blue) indicate low curvature and warm colors indicate high curvature (red) (EM tomogram range = 0.3 to 3.0 rad/µm, COMSOL model 0.1 to 0.9 rad/µm). (B) Representative images of computational model at the beginning, middle, and end of the power stroke (left panels). The panels on the left are model views (side and top views) of BB triplet MTs. The two panels on the right are graphs showing BB curvature for the BB proximal to distal axis (left) or for each triplet MT (right). The maximum value for each bin ($1/10^{th}$ the length of the BB) along the BB proximal-distal axis is normalized by subtracting the lowest maximum value of all bins in each BB. The graph represents the means and standard deviations of these

normalized maximum values for each proximal to distal bin (left) or each triplet MT (right). (C) Computational model components are depicted by the scaffolded model (left) and red inset shows the elements which represent structures present within and around *T. thermophila* cilia and BBs. Modeled structures include ciliary doublet MTs (cyan), central pair MTs (magenta), radial spokes (red), BB triplet MTs (blue), cartwheel (yellow), A-C linkers (grey), and BB-appendage MTs and SF (green) (Table 2). Representative image in the middle shows the computational model with the axial forces within the cilium and the cortical anchor points (magenta circles) of the BB, BB-appendage MTs (post-ciliary MTs) and SF. Representative image (right) of the separately added helical inner scaffold structure is shown in cyan, this structure is not included in any other computational models and its effect on BB MT curvature is quantified in Figure S3D with 4 nm and 8 nm beams. (D) Heatmaps show baseline model (left) at the end of the power stroke (Figures 3 and S3A-B) and parameter changes to this model. In each model, curvature is consistently increased at triplet MTs 5-6 above the SF attachment point. SF pulling (60nm) is the inverse of the manipulations made in later figures (Figure 4) and A-C linker and helical inner scaffold manipulations identify potential differences in curvature when BB triplet interconnectivity is disrupted. Additional parameter changes (perturbations) to this baseline model are described in Table 3 and Videos 3-10. Scale bar, 200 nm.

Figure S4. BBs display reversed bending patterns at 30°C compared to 37°C. (A) 30°C BBs exhibit different bending patterns from 37°C BBs, depending on where the cilium is in the beat stroke. Presentation and analysis as described in Figure S2. n = 9 BBs analyzed. (B) Heatmap indicates that the average curvature for the WT BBs at 30°C near the end of the power stroke. n = 5 BBs. (C) Standard deviation at end of power stroke average. (D) Averaged difference for BBs at 30°C versus 37°C. Black boxes denote >75% difference from other bins (p=>0.05). (E) BB curvature is more variable at 30°C than 37°C. 30°C BBs bend more in the negative direction and display wider range in distribution of positive or negative curvature in individual BBs (Mann-Whitney test: p=<0.01, F-test: p=<0.01). Data is represented as individual maximum

and minimum values from triplet MTs (dots), mean and quartiles of maximum values (boxes) and standard deviation (error bars). N = 9 BBs analyzed. Scale bar, 200 nm.

Figure S5. The striated fiber promotes focused BB bending. (A) *disA-1* BBs at 30°C display inconsistent bending patterns at the end of the power stroke. Presentation and analysis as described in Figure S2. n = 3 BBs analyzed. (B) WT and *disA-1* BBs exhibit unique bending profiles at the end of the ciliary power stroke. Top panel heatmaps compare the *disA-1* BB shown in the middle panel of Figure S5A to a matched WT BB. The heatmap on the left shows BB bending in a matched WT BB with the most similar cilia angle to the cilia of *disA-1* BBs analyzed at the end of the power stroke. The heatmap in the middle shows *disA-1* BB bending. The heatmap on the right quantifies the difference between the corresponding WT and *disA-1* BBs. Prominent differences between WT and *disA-1* BB bending are observed scattered across the BB. Black boxes denote >75% difference from other bins (p=>0.05). (C) Heatmaps compare the *disA-1* BB shown at the bottom panel of S5A to a matched WT BB. The heatmap on the left shows BB bending in a matched WT BB with the most similar cilia angle to the cilia of *disA-1* BBs analyzed. The heatmap in the middle shows *disA-1* BB bending. The heatmap on the right quantifies the difference between the corresponding WT and *disA-1* BBs. Prominent differences between WT and *disA-1* BB bending are observed scattered across the BB. The blue (negative) and red (positive) colors indicate the direction of curvature relative to the cell's anterior-posterior axis. Black boxes denote >75% difference from other bins (p=>0.05). (D) Heatmap indicates the average curvature for the disA-1 BBs at 30°C near the end of the power stroke. n = 3 BBs. (E) Standard deviation at end of power stroke average. (F) Average difference for *disA-1* and WT BBs near the end of the power stroke. Black boxes denote >75% difference from other bins (p=>0.05). Scale bar, 200 nm.

Figure S6. Poc1 promotes the distribution of bending between BB triplet MTs. (A) *poc1Δ* BBs display inconsistent triplet MT bending at the end of the power stroke. Presentation and analysis as described in Figure S2. n = 3 BBs analyzed. (B) WT and *poc1Δ* BBs exhibit differences at the beginning of the recovery stroke (near the end of

the power stroke). Top panel heatmaps compare the *poc1Δ* BB shown in the middle panel of S6A to a matched WT BB. The heatmap on the left shows BB bending in a matched WT BB with the most similar cilia angle to the cilia of *poc1Δ* BBs analyzed. The heatmap in the middle shows *poc1Δ* BB bending. The heatmap on the right quantifies the difference between the corresponding WT and *poc1Δ* BBs. Prominent differences between WT and *poc1Δ* BB bending at the bottom of triplet MTs 2, 6, and 7. Black boxes denote >75% difference from other bins (p=>0.05). (C) Heatmaps compare the *poc1Δ* BB shown in the bottom panel of S6A to a matched WT BB. The heatmap on the left shows BB bending in a matched WT BB with the most similar cilia angle to the cilia of *poc1Δ* BBs analyzed. The heatmap in the middle shows *poc1Δ* BB bending. The heatmap on the right quantifies the difference between the corresponding WT and *poc1Δ* BBs. Prominent differences between WT and *poc1Δ* BB bending at the middle of triplet MTs 5 and top of triplet MT 8. (D) *poc1Δ* BBs do not distribute bending well at the end of the power stroke and the beginning of the recovery stroke. The heatmap indicates that the average curvatures for the *poc1Δ* shown above (Figure S6A). Curvature is most prominent on triplet MT 5. (E) *poc1Δ* BBs bend have high standard deviation in curvature across the BB. The heatmap indicates the standard deviation in the *poc1Δ* BBs. The standard deviation is most prominent on triplet MT 5. (F) Average difference for *poc1Δ* and WT BBs near the end of the power stroke. Black boxes denote >75% difference from other bins (p=>0.05). (G) *poc1Δ* BBs asymmetrically lose triplet MTs (Meehl et al., 2016b). A section through a tomogram of the proximal region of a *poc1Δ* BB show the loss of triplet MTs 7-8. This is modeled in the right two panels showing that these triplet MTs are lost from the whole BB. This is consistent with the high and variable bending in triplet MTs 7-9 of the bottom BB shown in Figure S6A. (H) Graph shows the mean and standard deviation of triplet MT loss from *poc1Δ* BBs (Meehl et al., 2016b). Triplet MTs 1, 2, 7, 8, and 9 are most frequently lost. (H) Selected thin section images (450 acquired BBs) of *poc1Δ* BBs from cells grown at 38 °C. BBs show damage to MTs or an abnormal or wavy MT curvature. Scale bar, 200nm.

Figure S1

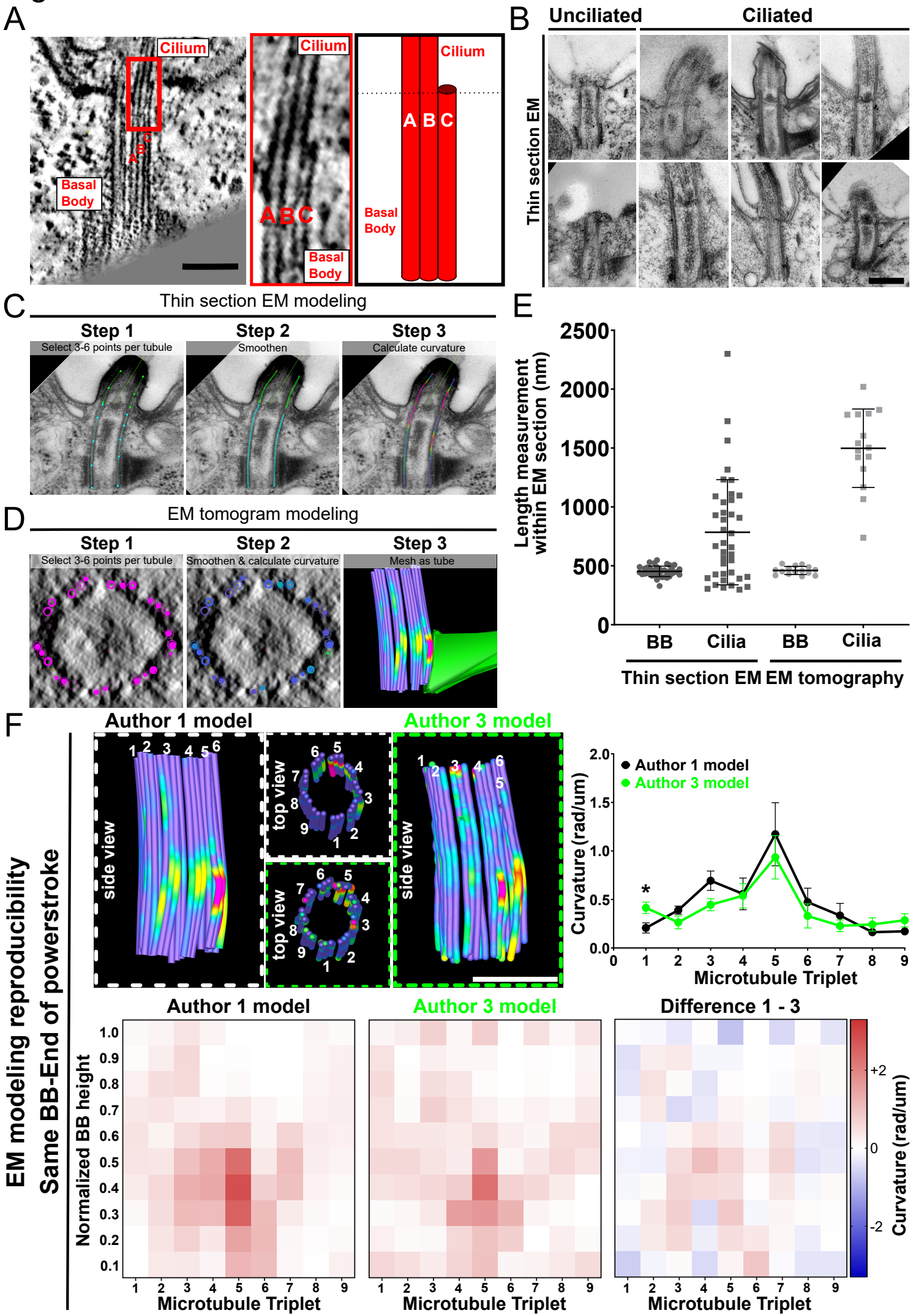
A
Cilium
Basal Body
A B C
ABC
B
Unciliated
Ciliated
Thin section EM
C
Thin section EM modeling
Step 1
Select 3-6 points per tubule
Step 2
Smoothen
Step 3
Calculate curvature
D
EM tomogram modeling
Step 1
Select 3-6 points per tubule
Step 2
Smoothen & calculate curvature
Step 3
Mesh as tube
E
Length measurement within EM section (nm)
2500
2000
1500
1000
500
0
BB
Cilia
BB
Cilia
Thin section EM
EM tomography
F
EM modeling reproducibility
Same BB-End of powerstroke
Author 1 model
Author 3 model
side view
top view
Curvature (rad/um)
Author 1 model
Author 3 model
Microtubule Triplet
Normalized BB height
Difference 1 - 3
+2
0
-2
Curvature (rad/um)

Figure S2

A

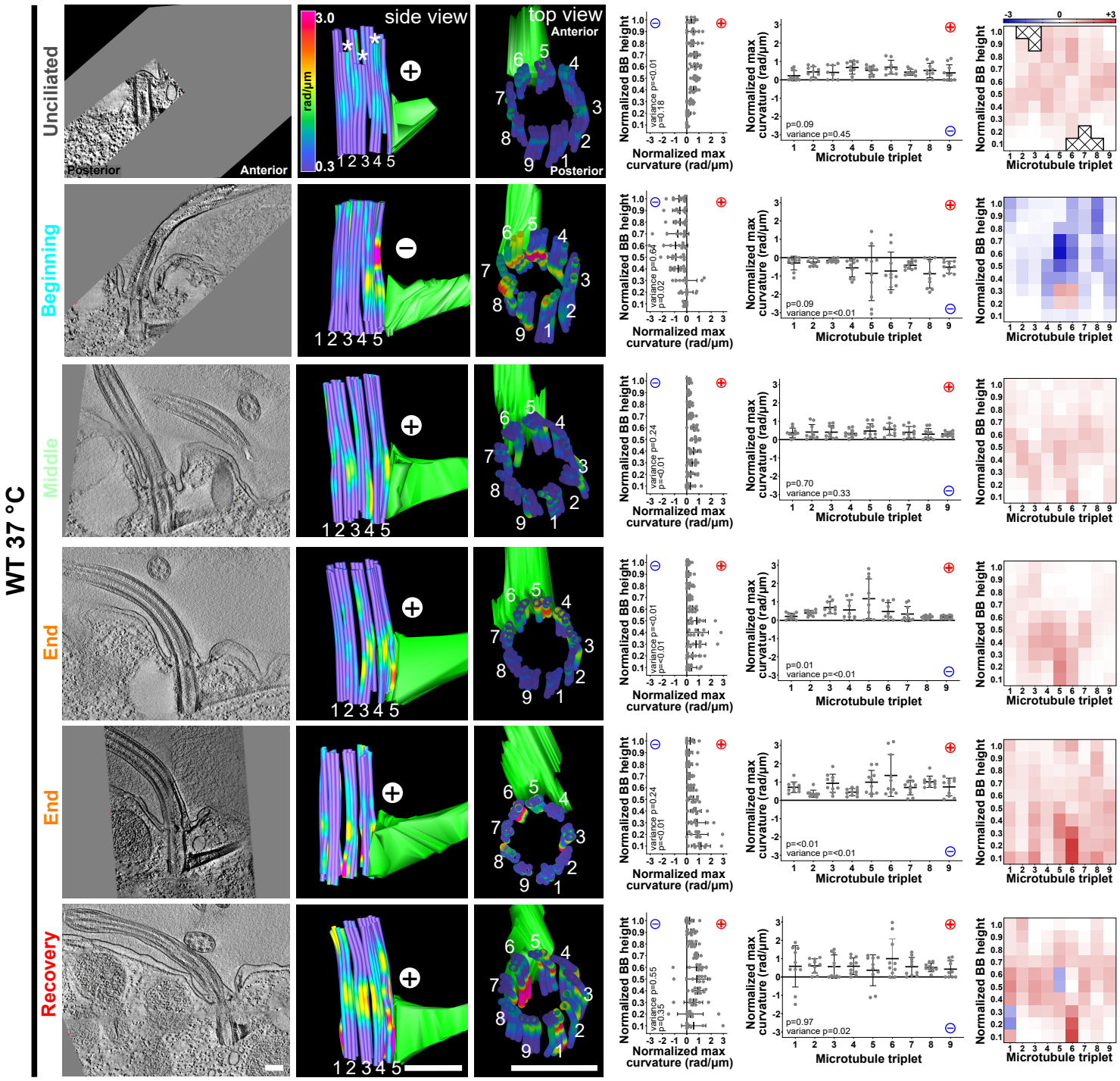

B

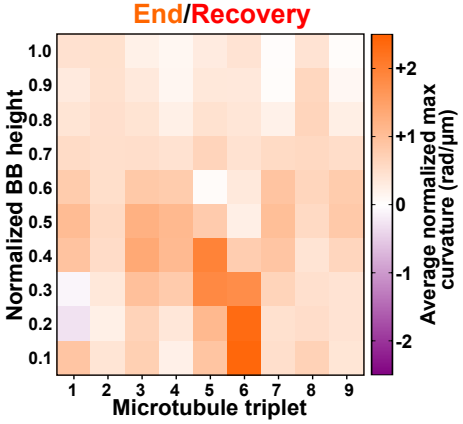

C

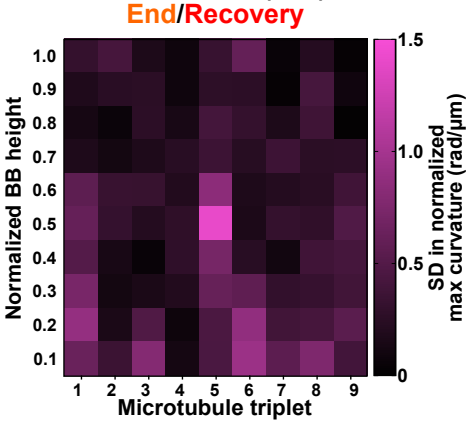

Figure S3

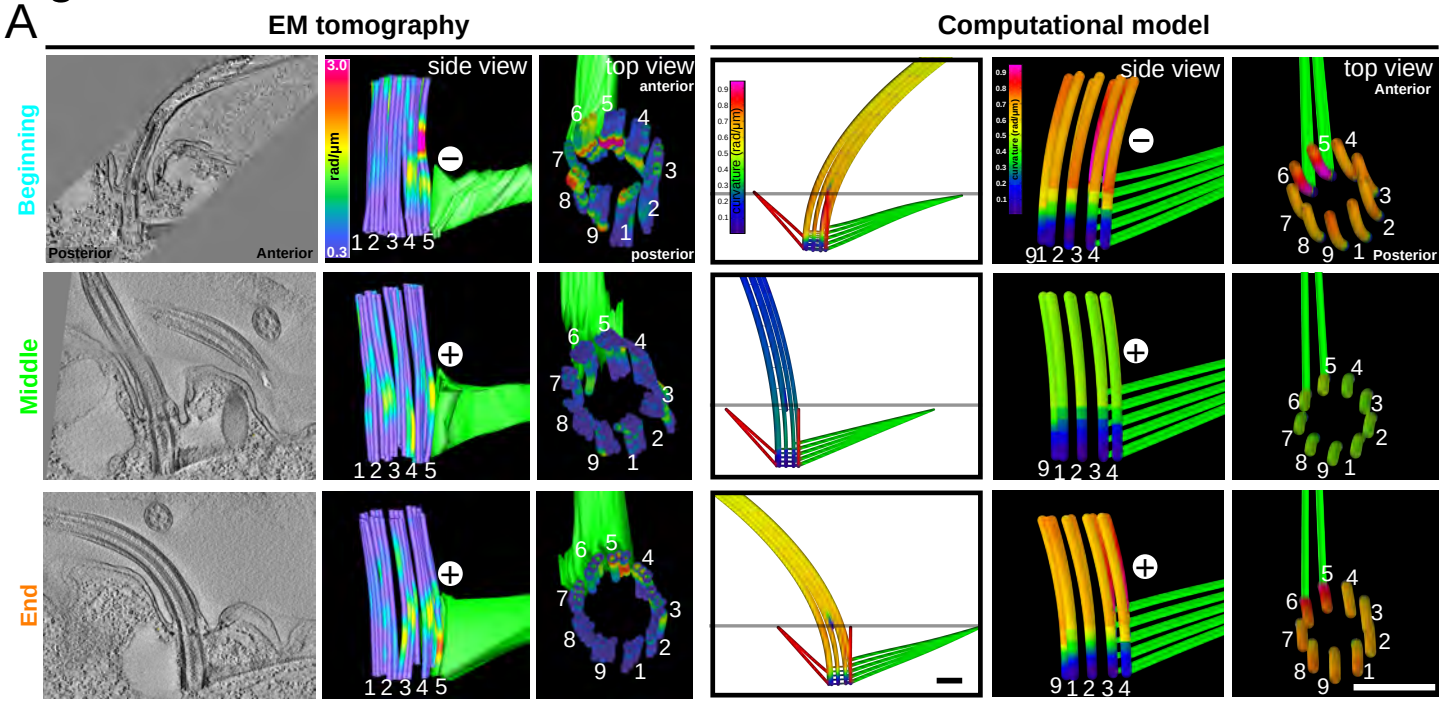
A
EM tomography
Computational model
Beginning
Middle
End
side view
top view
anterior
posterior
Posterior
Anterior
rad/μm
curvature (rad/μm)
1 2 3 4 5
9 1 2 3 4

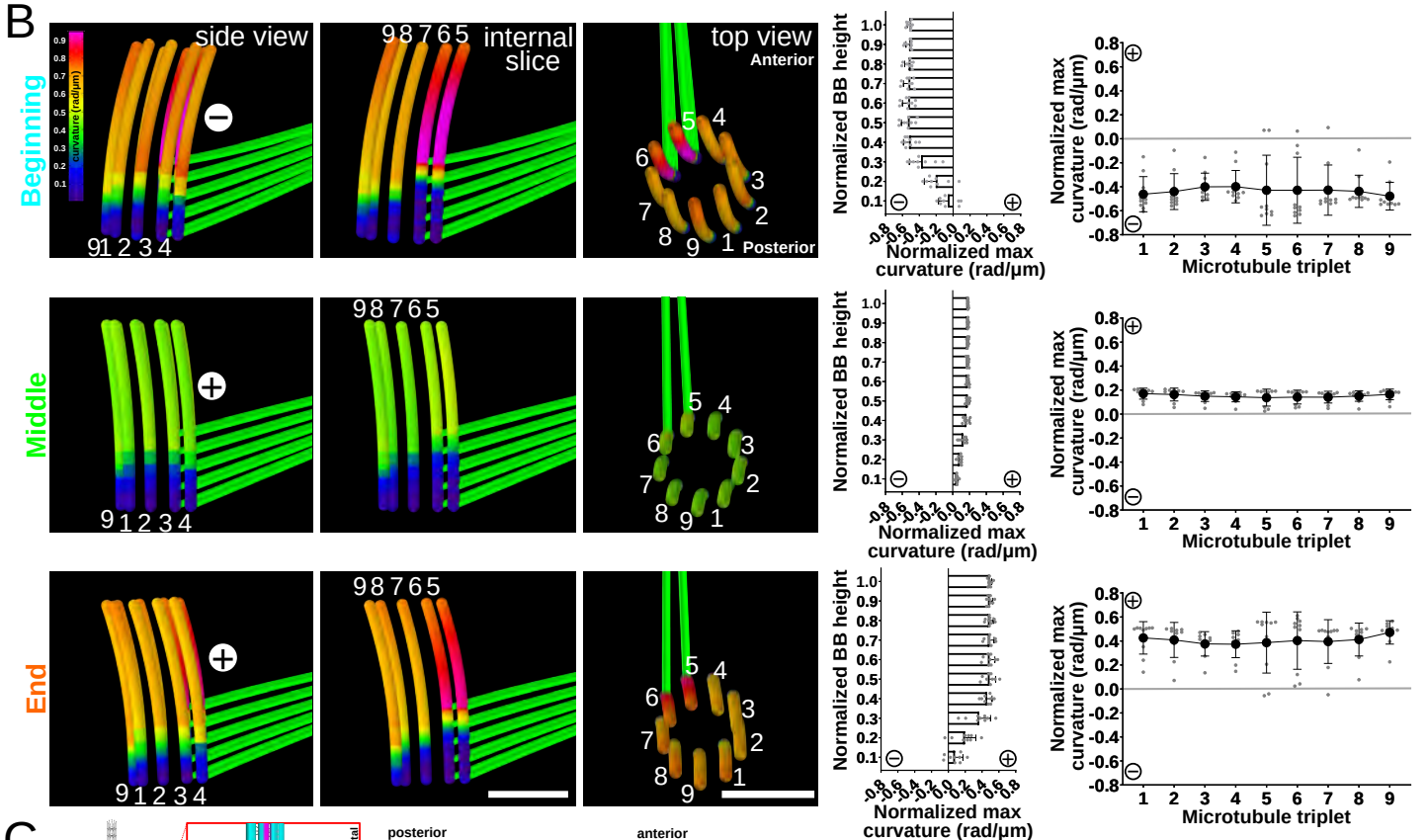
B
Beginning
Middle
End
side view
98765 internal slice
top view
Anterior
Posterior
curvature (rad/μm)
Normalized BB height
Normalized max curvature (rad/μm)
Microtubule triplet

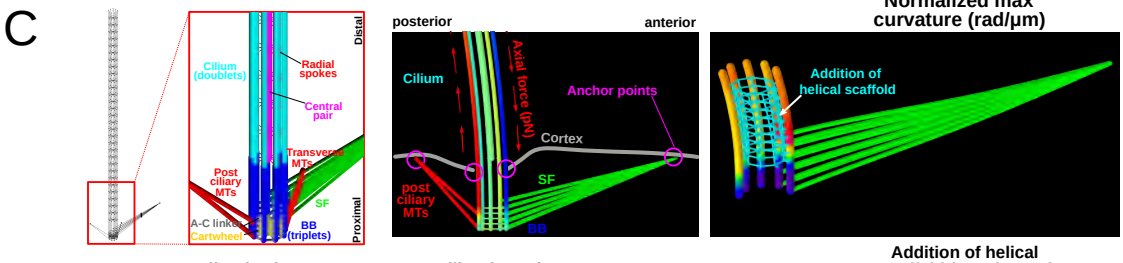
C
Cilium (doublets)
Radial spokes
Central pair
Transverse MTs
Post ciliary MTs
SF
BB (triplets)
A-C linker
Cartwheel
Distal
Proximal
posterior
anterior
Cilium
Axial force (pN)
Anchor points
Cortex
SF
post ciliary MTs
BB
Addition of helical scaffold

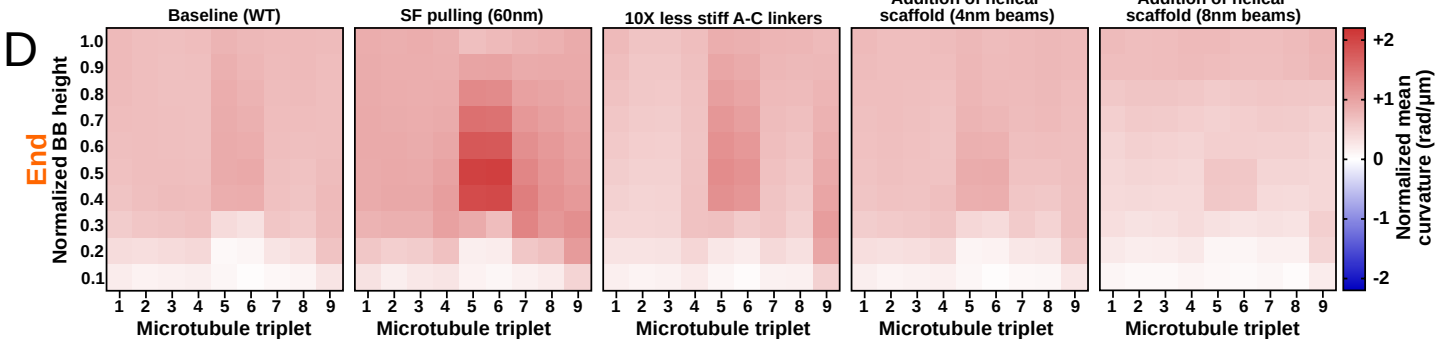
D
End
Baseline (WT)
SF pulling (60nm)
10X less stiff A-C linkers
Addition of helical scaffold (4nm beams)
Addition of helical scaffold (8nm beams)
Normalized BB height
Microtubule triplet
Normalized mean curvature (rad/μm)

Figure S4

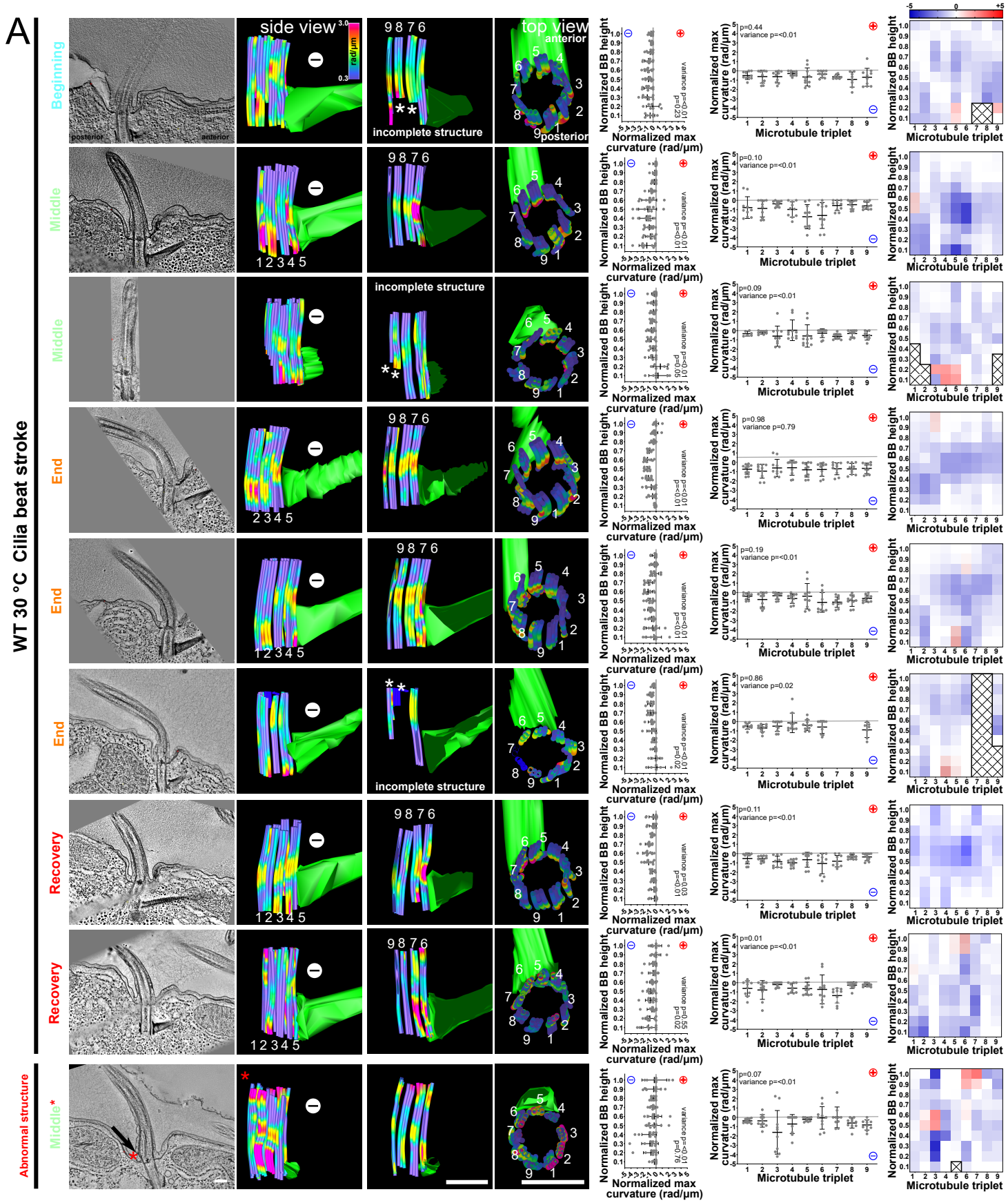
A
WT 30 °C Cilia beat stroke
Beginning
Middle
Middle
End
End
End
Recovery
Recovery
Abnormal structure
Middle*
side view
top view
anterior
posterior
incomplete structure
Normalized BB height
Normalized max curvature (rad/µm)
Microtubule triplet
Normalized max curvature (rad/µm)
B
Average curvature (n=5)
End/Recovery
Average normalized max curvature (rad/µm)
C
Standard deviation in curvature (n=5)
End/Recovery
SD in normalized max curvature (rad/µm)
D
Difference: average WT 30 °C - 37 °C
End/Recovery
Average normalized max curvature (rad/µm)
E
Range of normalized max curvature (rad/µm)
p=<0.01
variance p=<0.01
37°C
30°C

Figure S5

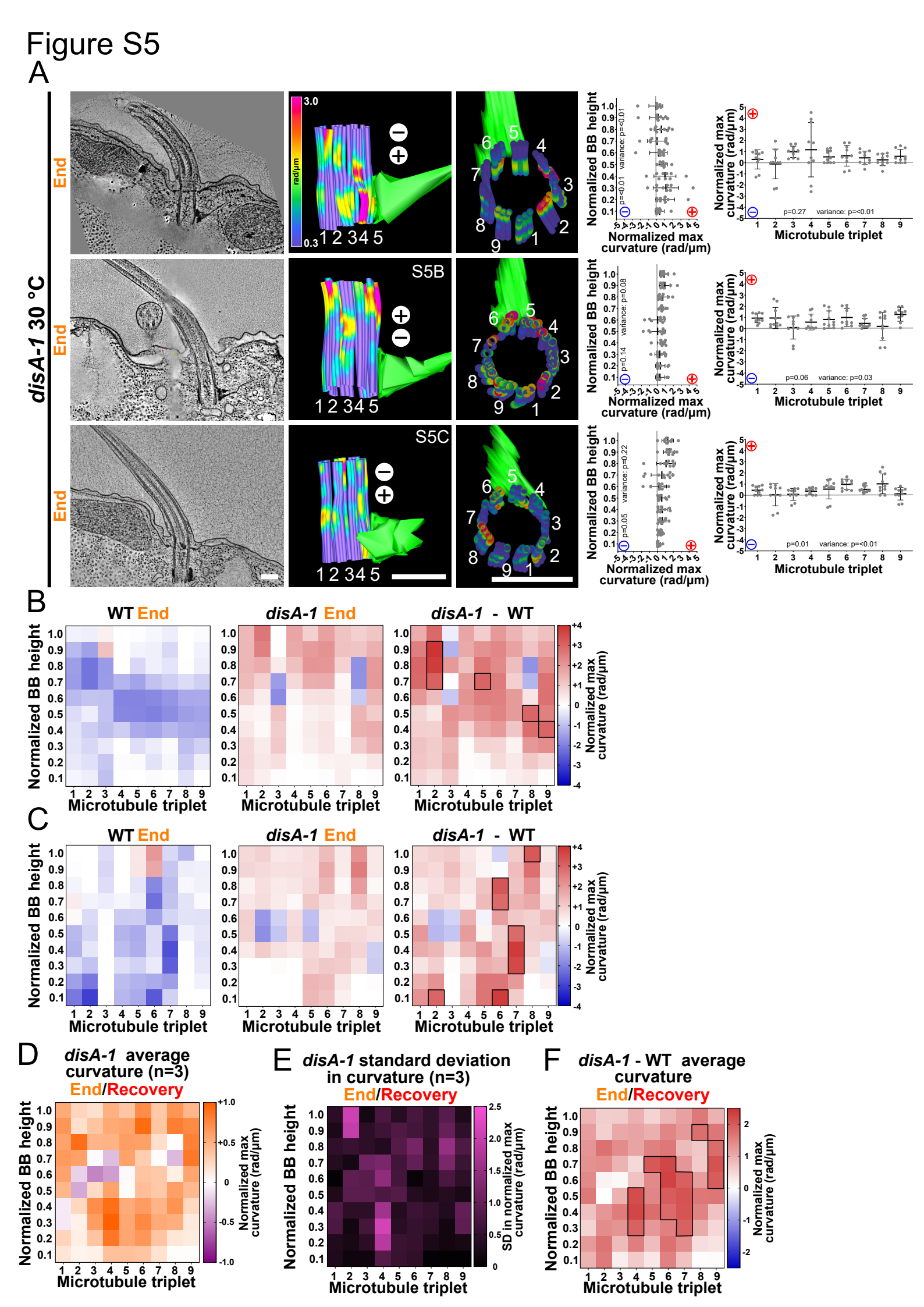
A
disA-1 30 °C
End
End
End
3.0
rad/µm
0.3
1 2 34 5
S5B
S5C
Normalized BB height
Normalized max curvature (rad/µm)
variance: p=<0.01
p=<0.01
variance: p=0.08
p=0.14
variance: p=0.22
p=0.05
Normalized max curvature (rad/µm)
Microtubule triplet
p=0.27
variance: p=<0.01
p=0.06
variance: p=0.03
p=0.01
variance: p=<0.01
B
WT End
disA-1 End
disA-1 - WT
Normalized BB height
Microtubule triplet
Normalized max curvature (rad/µm)
C
WT End
disA-1 End
disA-1 - WT
Normalized BB height
Microtubule triplet
Normalized max curvature (rad/µm)
D
disA-1 average curvature (n=3)
End/Recovery
Normalized BB height
Microtubule triplet
Normalized max curvature (rad/µm)
E
disA-1 standard deviation in curvature (n=3)
End/Recovery
Normalized BB height
Microtubule triplet
SD in normalized max curvature (rad/µm)
F
disA-1 - WT average curvature
End/Recovery
Normalized BB height
Microtubule triplet
Normalized max curvature (rad/µm)

Figure S6

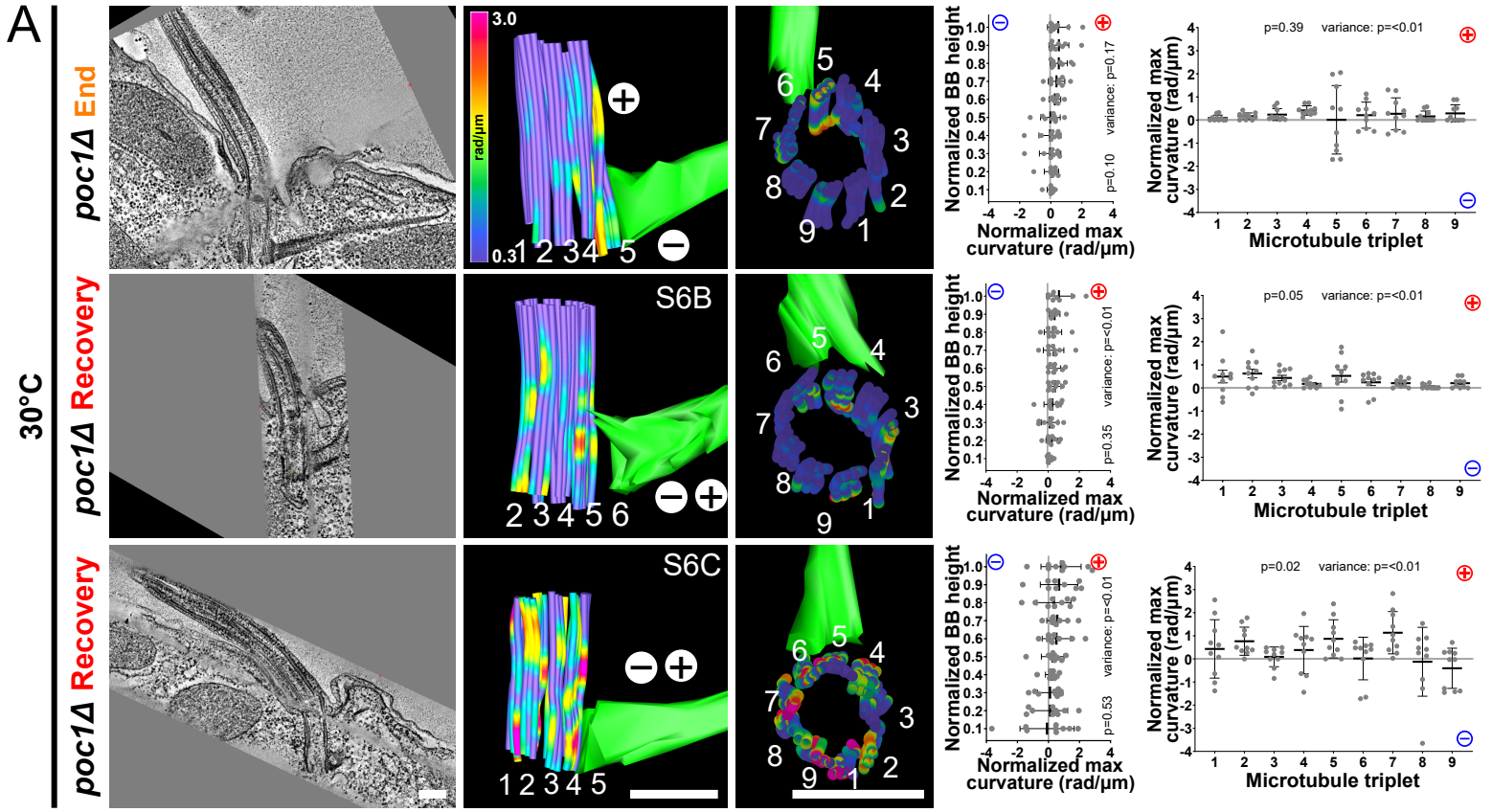
A
30°C
poc1Δ End
poc1Δ Recovery
poc1Δ Recovery
3.0
rad/µm
0.3
S6B
S6C
Normalized BB height
Normalized max curvature (rad/µm)
variance: p=0.17
p=0.10
variance: p=<0.01
variance: p=<0.01
p=0.35
variance: p=<0.01
variance: p=<0.01
p=0.53
p=0.39
variance: p=<0.01
p=0.05
variance: p=<0.01
p=0.02
variance: p=<0.01
Normalized max curvature (rad/µm)
Microtubule triplet

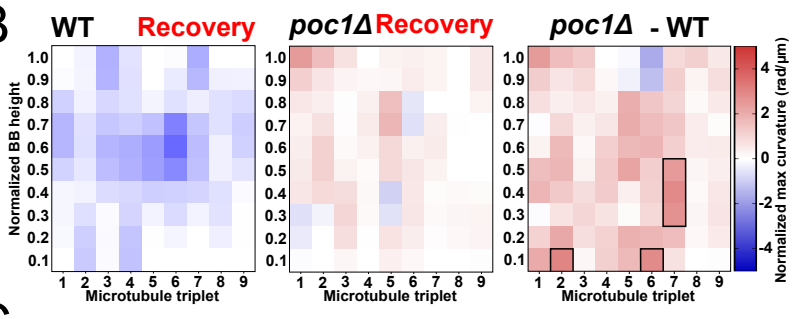
B
WT
Recovery
poc1ΔRecovery
poc1Δ - WT
Normalized BB height
Microtubule triplet
Normalized max curvature (rad/µm)

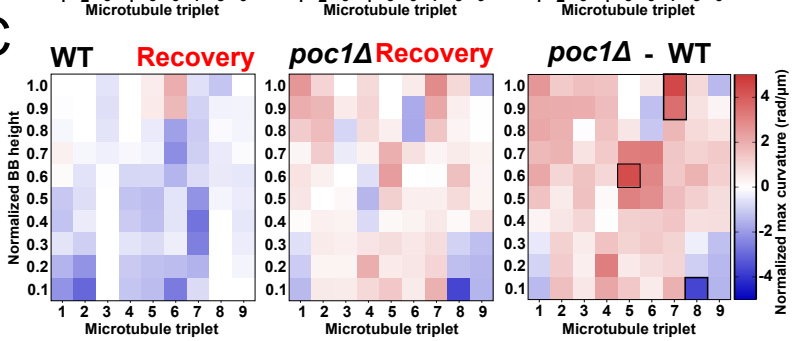
C
WT
Recovery
poc1ΔRecovery
poc1Δ - WT
Normalized BB height
Microtubule triplet
Normalized max curvature (rad/µm)

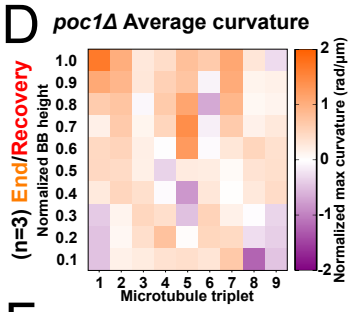
D
poc1Δ Average curvature
(n=3) End/Recovery
Normalized BB height
Microtubule triplet
Normalized max curvature (rad/µm)

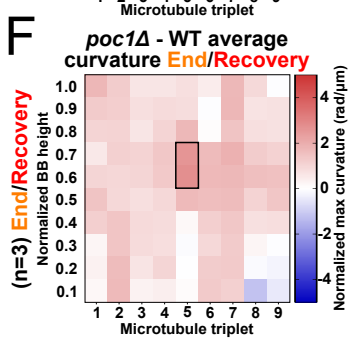
F
poc1Δ - WT average curvature End/Recovery
(n=3) End/Recovery
Normalized BB height
Microtubule triplet
Normalized max curvature (rad/µm)

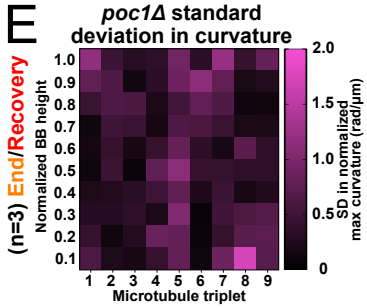
E
poc1Δ standard deviation in curvature
(n=3) End/Recovery
Normalized BB height
Microtubule triplet
SD in normalized max curvature (rad/µm)

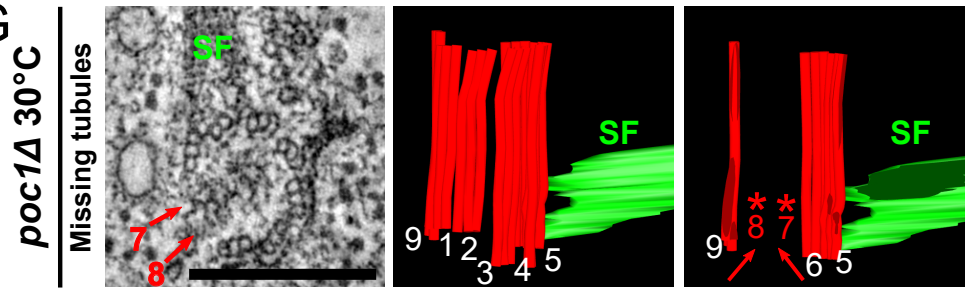
G
poc1Δ 30°C
Missing tubules
SF
SF
SF

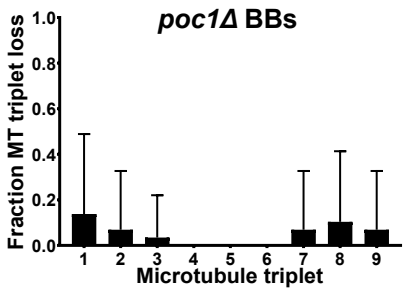
H
poc1Δ BBs
Fraction MT triplet loss
Microtubule triplet

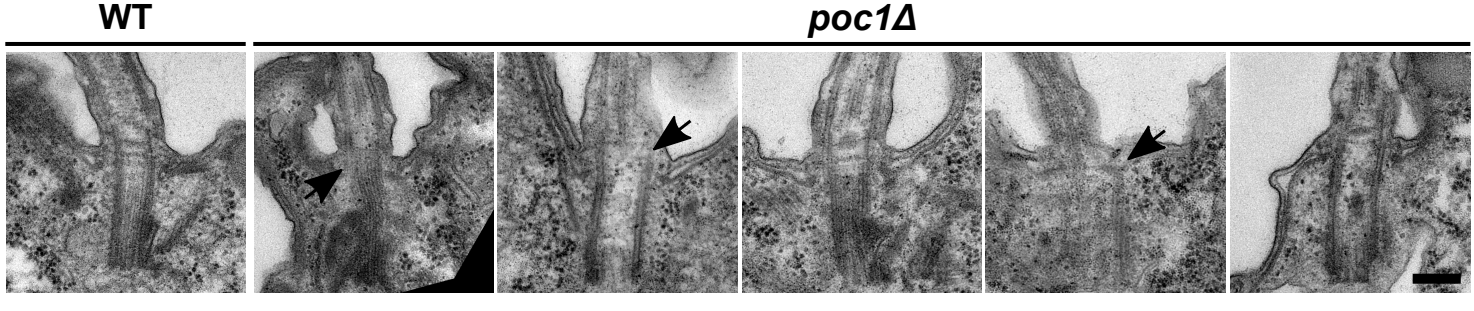
I
WT
poc1Δ
38°C - 48hrs